PHENOMENOLOGICAL ASPECTS OF CHIRAL SYMMETRY IN LATTICE GAUGE THEORY*

Anthony W. Thomas

Department of Physics and Mathematical Physics and
Special Research Centre for the Subatomic Structure of Matter
University of Adelaide, Australia 5005
e-mail: athomas@physics.adelaide.edu.au

(Received July 17, 2000)

The current limitations in computer speed mean that in order to compare lattice QCD simulations of hadron structure with data one must extrapolate from quark masses that are 5–10 times too large. In doing so it is vital that the constraints of chiral symmetry are correctly incorporated. We review some recent, exciting developments in our understanding of how to make these extrapolations.

PACS numbers: 12.38.Gc, 11.15.Ha

1. Introduction

The SU(2) axial current, $j^a_{\mu 5}$, is conserved in QCD with massless u and d quarks. As a consequence the axial charge, Q^a_5, commutes with the QCD Hamiltonian and one would expect a degenerate, opposite parity partner for each hadron. The absence of such states in the physical world implies that the vacuum must contain massless pseudoscalar mesons, known as Goldstone bosons. That is, SU(2) chiral symmetry is dynamically broken [1].

As we move away from the massless limit the Gell Mann–Oakes–Renner (GOR) relation tells us that

$$m_\pi^2 \propto \bar{m}, \qquad\qquad (\text{with} \quad \bar{m} = m_u = m_d \neq 0)\,. \tag{1}$$

Although this is, in principle, only guaranteed for quark masses, $\bar{m}$, near zero, lattice QCD calculations tell us that it holds over an enormous range, as high as $m_\pi \sim 1$ GeV. Rather than measuring the deviation from exact chiral symmetry using $\bar{m}$, which is scale dependent, we shall use m_π^2.

* Presented at the Meson 2000, Sixth International Workshop on Production, Properties and Interaction of Mesons, Cracow, Poland, May 19–23, 2000.

Current lattice calculations are typically restricted to pion masses larger than 500 MeV, with some pioneering work reporting preliminary results as low as 310 MeV. In order to compare these results with experimental data on hadron properties it is necessary to extrapolate the calculations at large pion masses to the physical value. In doing so it is crucial to respect the constraints imposed by chiral symmetry in QCD. In particular, as we discuss below, the existence of Goldstone bosons necessarily leads to behaviour which is not analytic in the quark mass. After reviewing the origin of this non-analytic structure we specifically examine the recent development of a method of extrapolation of hadron masses which respects the mathematical properties while building in the correct physics at large quark mass. The consequences of this for the sigma commutator are then reviewed. Following this we turn to recent results for baryon electromagnetic properties, before summarising.

2. Non-analytic behaviour

Spontaneous chiral symmetry breaking in QCD requires the existence of Goldstone bosons whose masses vanish in the limit of zero quark mass (the chiral limit). As a corollary to this, there must be contributions to hadron properties from Goldstone boson loops. These loops have the unique property that they give rise to terms in an expansion of most hadronic properties as a function of quark mass which are not analytic. As a simple example, consider the nucleon mass. The most important chiral corrections to M_N come from the processes $N \to N\pi \to N$ (σ_{NN}) and $N \to \Delta\pi \to N$ ($\sigma_{N\Delta}$). We write $M_N = M_N^{\rm bare} + \sigma_{NN} + \sigma_{N\Delta}$. In the heavy baryon limit one has

$$\sigma_{NN} = -\frac{3g_A^2}{16\pi^2 f_\pi^2} \int_0^\infty dk \frac{k^4 u^2(k)}{k^2 + m_\pi^2} \,. \tag{2}$$

Here $u(k)$ is a natural high momentum cut-off which is the Fourier transform of the source of the pion field (*e.g.* in the Cloudy Bag Model (CBM) it is $3j_1(kR)/kR$, with R the bag radius [3]). From the point of view of PCAC it is natural to identify $u(k)$ with the axial form-factor of the nucleon, a dipole with mass parameter 1.02 ± 0.08 GeV.

Quite independent of the form chosen for the ultra-violet cut-off, one finds that σ_{NN} is a non-analytic function of the quark mass. The non-analytic piece of σ_{NN} is independent of the form factor and gives

$$\sigma_{NN}^{\rm LNA} = -\frac{3g_A^2}{32\pi f_\pi^2} m_\pi^3 \sim \bar{m}^{\frac{3}{2}} \,. \tag{3}$$

This has a branch point, as a function of $\bar{m}$, at $\bar{m} = 0$. Such terms can only arise from Goldstone boson loops.

3. Chiral extrapolations of lattice data

It is natural to ask how significant this non-analytic behaviour is in practice. If the pion mass is given in GeV, $\sigma_{NN}^{\mathrm{LNA}} = -5.6 m_\pi^3$ and at the physical pion mass it is just -17 MeV. However, at only three times the physical pion mass, $m_\pi = 420$ MeV, it is -460 MeV — half the mass of the nucleon. If one's aim is to extract physical nucleon properties from lattice QCD calculations this is extremely important. The most sophisticated lattice calculations with dynamical fermions are only just becoming feasible at such low masses and to connect to the physical world one must extrapolate from $m_\pi \sim 500\,\mathrm{MeV}$ to $m_\pi = 140\,\mathrm{MeV}$. Clearly one must have control of the chiral behaviour.

Figure 1 shows recent lattice calculations of M_N as a function of m_π^2 from CP-PACS and UKQCD [4]. The dashed line indicates a fit which naively respects the presence of a LNA term,

$$M_N = \alpha + \beta m_\pi^2 + \gamma m_\pi^3 \,, \tag{4}$$

with α, β and γ fitted to the data. While this gives a very good fit to the data, the chiral coefficient γ is only -0.761, compared with the value -5.60 required by chiral symmetry. If one insists that γ be consistent with QCD the best fit one can obtain with this form is the dash-dot curve. This is clearly unacceptable.

An alternative suggested recently by Leinweber *et al.* [5], which also involves just three parameters, is to evaluate σ_{NN} and $\sigma_{N\Delta}$ with the same ultra-violet form factor, with mass parameter Λ, and to fit M_N as

$$M_N = \alpha + \beta m_\pi^2 + \sigma_{NN}(m_\pi, \Lambda) + \sigma_{N\Delta}(m_\pi, \Lambda) \,. \tag{5}$$

Using a sharp cut-off ($u(k) = \theta(\Lambda - k)$) these authors were able to obtain analytic expressions for σ_{NN} and $\sigma_{N\Delta}$ which reveal the correct LNA behaviour, and next to leading (NLNA) in the $\Delta\pi$ case, $\sigma_{N\Delta}^{\mathrm{NLNA}} \sim m_\pi^4 \ln m_\pi$. These expressions also reveal a branch point at $m_\pi = M_\Delta - M_N$, which is important if one is extrapolating from large values of m_π to the physical value. The solid curve in Fig. 1 is a two parameter fit to the lattice data using Eq. (5), but fixing Λ at a value suggested by CBM simulations to be equivalent to the preferred 1 GeV dipole. A small increase in Λ is necessary to fit the lowest mass data point, at $m_\pi^2 \sim 0.1$ GeV^2, but clearly one can describe the data very well while preserving the exact LNA and NLNA behaviour of QCD.

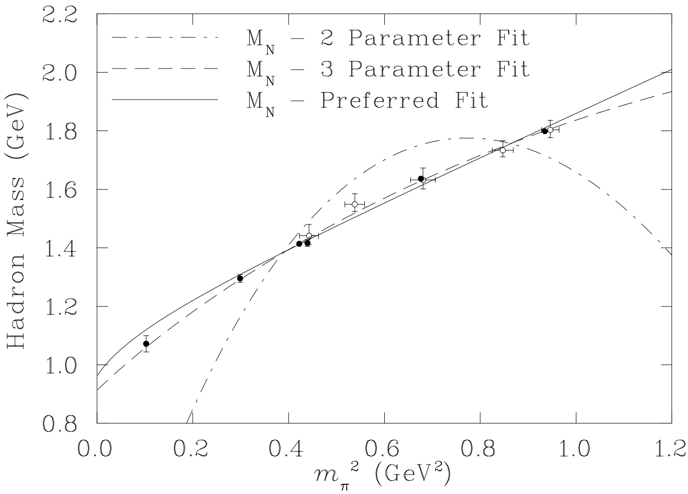

Fig. 1. A comparison between phenomenological fitting functions for the mass of the nucleon — from Ref. [5]. The two parameter fit corresponds to using Eq. (4) with γ set equal to the value known from χPT. The three parameter fit corresponds to letting γ vary as an unconstrained fit parameter. The solid line is the two parameter fit based on the functional form of Eq. (5).

4. The sigma commutator

The analysis of the lattice data for M_N, incorporating the correct non-analytic behaviour, can yield interesting new information concerning the sigma commutator of the nucleon:

$$\sigma_N = \frac{1}{3}\langle N|[Q_{i5},[Q_{i5},H_{\rm QCD}]]|N\rangle = \langle N|\bar{m}(\bar{u}u+\bar{d}d)|N\rangle\,. \tag{6}$$

This is a direct measure of chiral SU(2) symmetry breaking in QCD, and the widely accepted experimental value is $45\pm 8\,\text{MeV}$ [6]. (Although there are recent suggestions that it might be as much as 20 MeV larger [7].) Using the Feynman–Hellmann theorem one can also write

$$\sigma_N = \bar{m}\frac{\partial M_N}{\partial \bar{m}} = m_\pi^2 \frac{\partial M_N}{\partial m_\pi^2}\,. \tag{7}$$

Historically, lattice calculations have evaluated $\langle N|(\bar{u}u+\bar{d}d)|N\rangle$ at large quark mass and extrapolated this scale dependent quantity to the "physical" quark mass, which had to be determined in a separate calculation. The latest result with dynamical fermions, $\sigma_N = 18\pm 5$ MeV [8], illustrates how difficult this procedure is. On the other hand, if one has a fit to M_N as a function of m_π which is consistent with chiral symmetry, one can evaluate σ_N directly using Eq. (7). Using Eq. (5) with a sharp cut-off yields $\sigma_N \sim 55$ MeV, while a dipole form gives $\sigma_N \sim 45$ MeV [9]. The residual model dependence can only be removed by more accurate lattice data at low m_π^2. Nevertheless, the result $\sigma_N \in (45, 55)$ MeV is in very good agreement with the data. In contrast, the simple cubic fit, with γ inconsistent with chiral constraints, gives ~ 30 MeV. Until the experimental situation regarding σ_N improves, it is not possible to draw definite conclusions regarding the strangeness content of the nucleon. However, the fact that two-flavour QCD reproduces the current preferred value should certainly stimulate some thought and a lot of work.

5. Baryon electromagnetic properties

It is a completely general consequence of quantum mechanics that the long-range charge structure of the proton comes from its π^+ cloud ($p \to n\pi^+$), while for the neutron it comes from its π^- cloud ($n \to p\pi^-$). However it is not often realized that the LNA contribution to the nucleon charge radius goes like $\ln m_\pi$ and diverges as $\bar{m} \to 0$ [11]. This can never be described by a constituent quark model. Figure 2 shows the latest data from Mainz and Nikhef for the neutron electric form factor, in comparison with CBM calculations for a confinement radius between 0.9 and 1.0 fm. The long-range π^- tail of the neutron plays a crucial role.

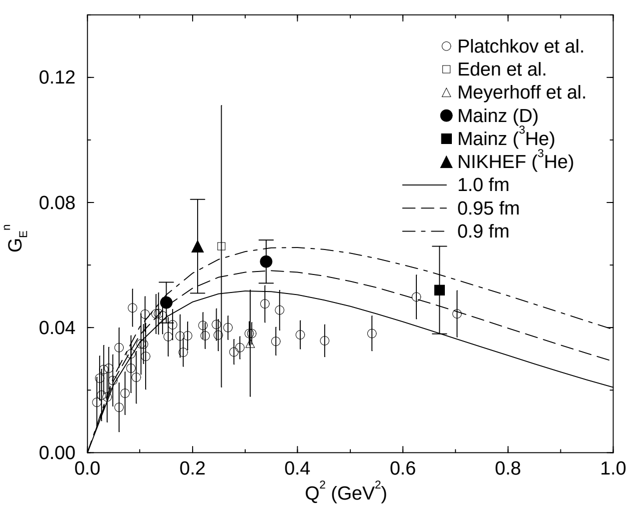

Fig. 2. Recent data for the neutron electric form factor in comparison with CBM calculations for a confining radius around 0.95fm — from Ref. [10].

While there is only limited (and indeed quite old) lattice data for hadron charge radii, recent experimental progress in the determination of hyperon charge radii has led us to examine the extrapolation procedure for obtaining charge data from the lattice simulations [12]. Figure 3 shows the extrapolation of the lattice data [13] for the charge radius of the proton. Clearly the agreement with experiment is much better once the chiral log required by chiral symmetry is correctly included, than if, for example, one simply made a linear extrapolation in the quark mass (or m_π^2). Full details of the results for all the octet baryons may be found in Ref. [12].

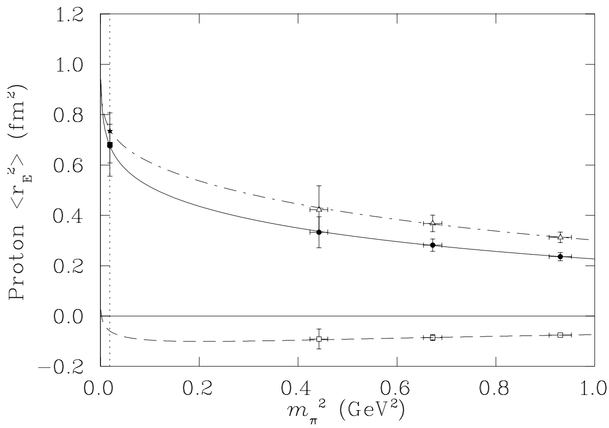

Fig. 3. Fits to lattice results for the squared electric charge radius of the proton — from Ref. [12]. Fits to the contributions from individual quark flavors are also shown: the u-quark sector results are indicated by open triangles and the d-quark sector results by open squares. Physical values predicted by the fits are indicated at the physical pion mass, where the full circle denotes the result predicted from the first extrapolation procedure and the full square denotes the baryon radius reconstructed from the individual quark flavor extrapolations. (*NB.* The latter values are actually so close as to be indistinguishable on the graph.) The experimental value is denoted by an asterisk.

The situation for baryon magnetic moments is also very interesting. The LNA contribution in this case arises from the diagram where the photon couples to the pion loop. As this involves two pion propagators the expansion of the proton and neutron moments is:

$$\mu^{p(n)} = \mu_0^{p(n)} \mp \alpha m_\pi + \mathcal{O}(m_\pi^2)\,. \tag{8}$$

Here $\mu_0^{p(n)}$ is the value in the chiral limit and the linear term in m_π is proportional to $\bar{m}^{\frac{1}{2}}$, a branch point at $\bar{m} = 0$. The coefficient of the LNA term is $\alpha = 4.4\mu_N$ GeV^{-1}. At the physical pion mass this LNA contribution is $0.6\mu_N$, which is almost a third of the neutron magnetic moment. *No constituent quark model can or should get better agreement with data than this.*

Just as for M_N, the chiral behaviour of $\mu^{p(n)}$ is vital to a correct extrapolation of lattice data. One can obtain a very satisfactory fit to some rather old data, which happens to be the best available, using the simple Padé [14]:

$$\mu^{p(n)} = \frac{\mu_0^{p(n)}}{1 \pm \frac{\alpha}{\mu_0^{p(n)}} m_\pi + \beta m_\pi^2} \, . \tag{9}$$

The data can only determine two parameters and Eq. (9) has just two free parameters while guaranteeing the correct LNA behaviour as $m_\pi \to 0$ **and** the correct behaviour of HQET at large m_π^2. The extrapolated values of μ^p and μ^n at the physical pion mass, $2.85 \pm 0.22 \mu_N$ and $-1.90 \pm 0.15 \mu_N$ are currently the best estimates from non-perturbative QCD [14]. For more details of this fit we refer to Ref. [14], while the application of similar ideas to other members of the nucleon octet we refer to Ref. [15], and for the strangeness magnetic moment of the nucleon we refer to Ref. [16].

Incidentally, from the point of view of the naive quark model it is interesting to plot the ratio of the proton to neutron magnetic moments as a function of m_π^2. The closeness of the experimental value to $-3/2$ is usually taken as a major success. However, we see from Fig. 4 that it is in fact a matter of luck! We stress that the large slope of the ratio near $m_\pi^2 = 0$ is *model independent.*

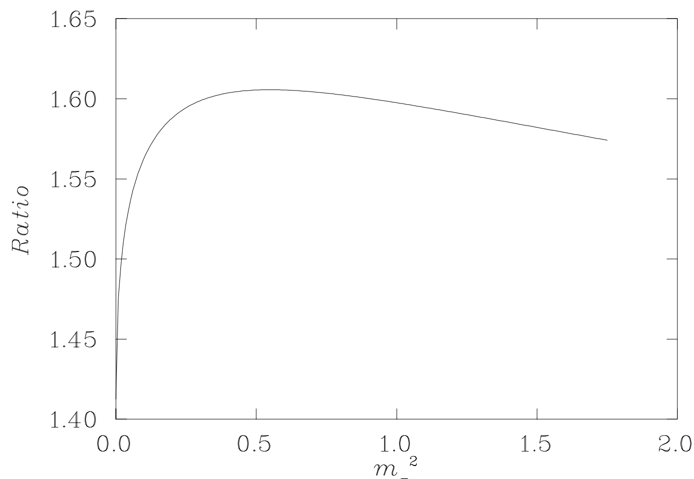

Fig. 4. Ratio of the proton to neutron magnetic moments as a function of m_π^2 obtained from the Padé approximants in Eq. (9). We stress that the behaviour as $m_\pi^2 \to 0$ is *model independent.*

6. Conclusion

In the region of quark masses $\bar{m} > 60$ MeV or so (m_π greater than typically 400–500 MeV) lattice QCD suggests that hadron properties are smooth, slowly varying functions of something like a constituent quark mass, $M \sim M_0 + c\bar{m}$ (with $c \sim 1$). Indeed, $M_N \sim 3M, M_{\rho,\omega} \sim 2M$ and magnetic moments behave like $1/M$. But as $\bar{m}$ decreases below this scale chiral symmetry leads to rapid, non-analytic variation, with $\delta M_N \sim \bar{m}^{3/2}, \delta\mu_H \sim \bar{m}^{1/2}$ and $\delta < r^2 >_{\rm ch} \sim \ln \bar{m}$.

Chiral quark models like the cloudy bag provide a natural explanation of this transition. The scale is basically set by the inverse size of the pion source – the inverse of the bag radius in the bag model. As practical consequences of this understanding we have shown:

- the best values of the proton and neutron magnetic moments from QCD;
- the best value of the sigma commutator;
- improved values for the charge radii of the baryon octet;
- improved values for the magnetic moments of the hyperons.

In addition, although we did not have time to discuss it, this approach has led to the best current value for the strangeness magnetic moment of the proton from lattice QCD, $G_M^s = -0.16 \pm 0.18\mu_N$ [16].

Clearly, while much has been achieved, even more remains to be done. It is vital that lattice calculations with dynamical fermions are pushed to the lowest possible quark masses, taking advantage of developments of improved actions and so on. It is also vital to further develop our understanding of the physics of chiral extrapolation by comparison with these new calculations, by looking at new applications and by further comparison with chiral models.

It is a pleasure to thank my collaborators in this work, especially Emily Hackett-Jones, Derek Leinweber, Dinghui Lu, Kazuo Tsushima and Stewart Wright for their part in the development of my understanding of this fascinating problem. I would also like to thank Will Detmold for a careful reading of the manuscript. This work was supported by the Australian Research Council and the University of Adelaide.

REFERENCES

[1] H. Pagels, *Phys. Rep.* **16**, 219 (1975).

[2] J.N. Labrenz, S.R. Sharpe, *Phys. Rev.* **D54**, 4595 (1996).

[3] S. Theberge, A.W. Thomas, G.A. Miller, *Phys. Rev.* **D22**, 2838 (1980); A.W. Thomas, *Adv. Nucl. Phys.* **13**, 1 (1984).

[4] S. Aoki *et al.* [CP-PACS], *Phys. Rev.* **D60**, 114508 (1999); C.R. Allton *et al.* [UKQCD], *Phys. Rev.* **D60**, 034507 (1999).

[5] D.B. Leinweber *et al.*, *Phys. Rev.* **D61**, 074502 (2000).

[6] J. Gasser, H. Leutwyler, M. E. Sainio, *Phys. Lett.* **B253**, 252 (1991).

[7] M. Knecht, `hep-ph/9912443`.

[8] SESAM Collaboration, S. Gusken *et al.*, *Phys. Rev.* **D59**, 054504 (1999).

[9] D.B. Leinweber *et al.*, *Phys. Lett.* **B482**, 109 (2000).

[10] D.H. Lu *et al.*, in Proc. Int. Conf. Few Body Problems, Taipei, 2000, to appear in *Nucl. Phys.* **A**; D.H. Lu *et al.*, *Phys. Rev.* **C60**, 068201 (1999.

[11] D.B. Leinweber, T.D. Cohen, *Phys. Rev.* **D47**, 2147 (1993).

[12] E.J. Hackett-Jones, D.B. Leinweber, A.W. Thomas, Incorporating Chiral Symmetry and Heavy Quark Effective Theory in Extrapolations of Octet Baryon Charge Radii, University of Adelaide preprint, ADP-00-38/T421 (2000).

[13] D.B. Leinweber, R.M. Woloshyn, T. Draper, *Phys. Rev.* **D43**, 1659 (1991).

[14] D.B. Leinweber *et al.*, *Phys. Rev.* **D60**, 034014 (1999).

[15] E.J. Hackett-Jones, D.B. Leinweber, A.W. Thomas, `hep-lat/0004006`.

[16] D.B. Leinweber, A.W. Thomas, `hep-lat/9912052`.